The case for a dynamical subsurface ecosystem

C. Magnabosco*[1,2], P.H.A. Timmers[3], M.C.Y. Lau[1], G. Borgonie[4,5], B. Linage-Alvarez[4], O. Kuloyo[4,6], R. Alleva[1], T.L. Kieft[8], G.S. Slater[9], E. van Heerden[4], B. Sherwood Lollar[10], and T.C. Onstott[1]

[1]Princeton University; Princeton USA
[2]Massachusetts Institute of Technology; Cambridge USA
[3]Wageningen University; Wageningen Netherlands
[4]University of the Free State; Bloemfontein South Africa
[5]Extreme Life Isyensya; Gentbrugge Belgium
[6]University of Calgary; Calgary Canada
[8]New Mexico Institute of Mining and Technology; Socorro USA
[9]McMaster University; Hamilton Canada
[10]University of Toronto; Toronto Canada

The introduction and concentration of electron donors and acceptors in the subsurface biosphere is controlled by the mixing of subsurface fluids[1], but the mechanisms and rates at which microbial communities respond to changes induced by fluid mixing and transport are relatively unknown. Subsurface microbial ecosystems whose estimated doubling times range from <1 to >3,000 years[2, 3, 4, 5, 6, 7, 8] are often considered to be relatively static. Despite marked changes in geochemistry over a 1-year period[9, 10], the bacterial community inhabiting a 1339 m below land surface (mbls) fracture (Be326) remained largely unchanged[9] and exhibited PLFA isotopic signatures consistent with the accumulation of ^{13}C-DIC impacted by the microbial oxidation of CH_4[10]. These CH_4 oxidizing (MO) bacteria and archaea are an essential link between the Be326 subsurface carbon cycle and microbial community[10] and were hypothesized to contain members of the community that are most sensitive to environmental change. To evaluate this hypothesis, we used a combination of high throughput sequence analysis methods (DNA, RNA, and protein) and geochemical monitoring of Be326's in situ fracture fluids over the course of both longer (2.5 year) and shorter (2-week) timescales and validated our findings through a series of ^{13}C-CH_4 laboratory enrichment experiments.

*Please direct communication to: cm13@princeton.edu

We show that Be326's MO organisms responded to changes in electron donor and acceptor availability in their natural subsurface habitat and under laboratory conditions over extended periods of time. These results provide the most definitive evidence to date that, like the marine subsurface[4], CH_4 oxidation occurs and is an integral component of the deep terrestrial subsurface carbon cycle. Further, the responsiveness of this component of the microbial community to changes in geochemistry illustrates a more dynamic subsurface ecosystem than previously understood.

Throughout a 2.5-year sampling period at Be326, δ^2H and δ^{18}O isotopic signatures of the fracture fluid over the 3 sampling points (Figure 1) indicated significant changes in the nature of the fluids over time. In 2011 (the first sampling point), the fluids were dominated by paleometeoric fluids and were consistent with other fluids located approximately 1,000 to 1,500 mbls in the Witwatersrand Formation (South Africa)[1, 11]. In 2012 and 2013, δ^{18}O and δ^2H signatures were displaced significantly above the Global Meteoric Water Line[12] (GMWL) in a pattern well-established to be consistent with mixing with older more highly altered fluids[13]. Mixing with contamination fluids such as mine service water would have resulted in a different displacement pattern – ruling out the possibility that the geochemical or microbial shifts in the borehole over time were related to contamination. Instead, this pattern indicates an increased component of ancient *in situ* fracture fluids in the borehole over time (Supplementary Discussion).

Geophysical-chemical measurements were made for both the 2.5-year and 2-week time series (Table 1). For the two time series, the mean and variance of temperature, pH, and CH_4 concentration measurements were relatively similar whereas the degree and magnitude to which E_h, SO_4^{2-}, NO_3^-, and H_2 concentrations changed was much greater over the 2.5-year time series. Within the 2.5-year time series, the fracture fluids shifted from a more reducing environment ($2011_{Eh} = -98$ mV, $2011_{[H2]} = 130$ nM) with limited electron acceptor availability ($2011_{[Sulph.]} = 37$ μM, $2011_{[Nitr.]} = 0.4$ μM) to a more oxidizing ($2013_{Eh} = 21 \pm 28$ mV, $2013_{[H2]} = 25$ nM) environment with much greater electron acceptor availability ($2013_{[Sulph.]} = 479$ μM, $2013_{[Nitr.]} = 4.5$ μM). The 2-week time series did not exhibit as large of a shift in electron-acceptor availability as the 2.5-year time series and maintained a positive E_h throughout (Table 1).

As the organisms responsible for MO in Be326 were reported to be present at relatively low abundances[10] , a targeted assembly pipeline[1] based on the PRICE assembler[14] was implemented to assemble methyl-coenzyme M reductase (*mcrA*) – the protein encoding gene (PEG) responsible for the first step in the anaerobic oxidation of methane (AOM)[15] – and a suite of CH_4 monooxygenases (*mmo*) that are known to play a role in the aerobic oxidation of methane[16]. This pipeline was applied to sets of metagenomic and metatranscriptomic data collected over a 2.5-year period (designated as the 2011, 2012, 2013 samples) and an additional set of metatranscriptomic data that spanned a 2-week

[1] https://github.com/cmagnabosco/OmicPipelines

2.5-year Time Series	**2011**	**2012**	**2013**
Dates Sampled	Jan 21-27, 2011	July 12-27, 2012	Aug 1-15, 2013
Temperature (^{o}C)	36.9	37.3 ± 1.2	35.1 ± 0.8
pH	8.83	8.55	8.17 ± 0.7
E_h (mV)	-98	-27.5 ± 6.4	21 ± 28
SO_4^{2-} (μM)	137	623	479
NO_3^- (μM)	0.4	4.4	4.5
O_2 (Chemet) (μM)	b.d.	9.3	b.d.*
H_2 (nM)	130	9	25
CH_4 (mM)	2.0	0.9	1.1

2-week Time Series	**T_0**	**T_1**	**T_2**
Dates Sampled	Aug 1, 2013	Aug 8, 2013	Aug 15, 2013
Temperature (^{o}C)	35.8	35.3	28.6
pH	8.2	8.1	7.9
E_h (mV)	9	53	1
SO_4^{2-} (μM)	531	499	459
NO_3^- (μM)	5.3	5.3	3.7
O_2 (Chemet) (μM)	b.d.*	b.d.*	b.d.*
H_2 (nM)	5.8×10^{-5}	10.4	39.8
CH_4 (mM)	0.8	1.2	1.0

Table 1: **Geophysical-chemical measurements from the 2.5-year and 2-week time series**. b.d. ≤ 0.31 μM; b.d.* ≤ 1.6 μM

period in 2013 (designated as the T_0, T_1, T_2 samples). Notably, *mcrA* was selected as an indicator for anaerobic methane oxidizers (ANME) because, phylogenetically, it corresponds with the 16S phylogeny of ANME (and methanogens) and their corresponding AOM (methanogenic) pathways[17]. Metaproteomic data were generated and mapped to the collection of assembled PEGs and a database of other known McrA and MMO peptide sequences (Supplementary Data 1) to confirm the presence of assembled PEGs. The relative abundances of 16S rRNA transcripts were also calculated from the total metatranscriptomic data as described in the Supplementary Methods.

Following targeted assembly and annotation, two complete *mcrA* PEGs related to ANME-1 and "*Ca.* Methanoperedens" (ANME-2d) were assembled while only one complete *mmo* PEG closely related to *Methylococcus capsulatus* was recovered from the metagenomic and metatranscriptomic data (Figure 2, Supplementary Data 2). Partial *mcrA* PEGs related to Methanomicrobia and Methanobacteria were also identified in the high-throughput data (Figure 2, Supplementary Data 2), but partially assembled mmo-related PEGs were omitted in downstream analyses due to the difficulty in distinguishing mmo from

homologous ammonia monooxygenase PEGs[18]. The predicted proteins (Supplementary Data 3) from the assembled ANME-1, "*Ca.* Methanoperedens", and *Methylococcus* PEGs were all identified within the metaproteomic data (Supplementary Data 4) and further confirm the presence and activity of these groups of organisms.

The relative abundance (based on coverage) of each PEG was calculated using Bowtie2[19] (-very-sensitive-local; Supplementary Methods) and indicated that the dominant members of the MO community in the metagenomes and metatranscriptomes changed over the 2.5-year time series (Figure 2) but remained constant during the 2-week time series (Table 2). These observations were consistent with the relative changes in geochemistry over both time scales (Table 1). In fact, the relative transcript abundances of MO members throughout the long-term time series were tightly correlated to changes in geochemistry (Tables 3, 4). In particular, ANME-1 transcript abundances were positively correlated to CH_4 ($R^2_{16S} = 0.96$, $R^2_{mcrA} = 0.99$) and H_2 ($R^2_{16S} = 0.98$, $R^2_{mcrA} = 0.98$) while "Ca. Methanoperedens" transcript abundances were positively correlated to E_h ($R^2_{16S} = 0.99$, $R^2_{mcrA} = 0.99$) and pH ($R^2_{16S} = 0.96$, $R^2_{mcrA} = 0.99$). O_2 concentrations in 2011 and 2013 were below detection (Table 1) but detected in 2012 (9.3 μM). Similarly, the aerobic *Methylococcus*-related MO exhibited maximum transcript abundance in 2012 (Figure 1, Supplementary Discussion) and may have been positively correlated to O_2 concentrations over time. "Ca. Methanoperedens" was the dominant member ($73.3 \pm 2.8\%$) of the MO community during the 2-week time series (Table 2) when fracture fluids contained high concentrations of SO_4^{2-} (496 ± 36 μM) and NO_3^- (4.8 ± 0.9 μM) along with a positive E_h (21 ± 28 mV).

	2011	**2012**	**2013**	$\mathbf{T_0^\star}$	$\mathbf{T_1^\star}$	$\mathbf{T_2^\star}$
ANME-1	90.21; 98.71	20.55; 17.93	16.94; 40.45	26.82	29.43	23.70
"Ca. M-peredens"	0.79; 0.00	38.20; 25.48	83.06; 52.34	73.18	70.57	76.10
M-microbia	0.00; 0.00	8.71; 8.87	0.00; 0.00	0.00	0.00	0.00
M-bacteria	0.00; 1.14	0.00; 5.04	0.00; 0.00	0.00	0.00	0.00
M. capusulatus	9.00; 0.15	32.54; 42.67	0.00; 7.21	0.00	0.00	0.21

Table 2: **Change in the CH_4 community and expression.** This table displays the relative abundance (%) of each taxa's with respect to their CH_4-related protein encoding gene (*mcrA* or *mmo*) abundance relative to the total methane oxidizer (MO) and methanogen community (DNA abundance; RNA abundance). The $\star$ next to T_0, T_1, and T_2 signify that only RNA abundances are reported."Ca. M-peredens"="*Ca.* Methanoperedens"; M-microbia=Methanomicrobia; M-bacteria=Methanobacteria; M. capsulatus=*Methylococcus capsulatus*.

To better understand the response of the MO community to changes in electron donor and acceptor balance, two sets of ^{13}C-CH_4 laboratory enrichment experiments were performed on fracture water collected in 2012 and 2013 (Supplementary Methods). As ANME−

		NO_3^-	SO_4^{2-}	CH_4	E_h	pH	H_2
2.5-Year Time-Series	"*Ca.* Methanoperedens"	0.79	0.76	-0.82	0.99	-0.98	-0.86
	ANME-1	-0.97	-0.96	0.98	-0.91	0.81	0.99
	Methylococcales	0.45	0.49	-0.40	-0.20	0.39	-0.33
2-Week Time-Series	"*Ca.* Methanoperedens"	0.51	0.84	-0.86	-0.36	0.77	-0.71
	ANME-1	0.55	0.87	-0.83	-0.31	0.80	-0.75
	Methylococcales	0.51	0.84	-0.86	-0.36	0.77	-0.71

Table 3: **Correlation (Pearson's r) between taxa RNA abundance (determined by 16S) and geochemical parameters**. The R^2_{16S} values reported in the main text are the square of the values reported above.

		NO_3^-	SO_4^{2-}	CH_4	E_h	pH	H_2
2.5-Year Time-Series	"*Ca.* Methanoperedens"	0.70	0.67	-0.75	0.99	-0.99	-0.79
	ANME-1	-0.99	-0.99	0.99	-0.77	0.63	0.99
	Methylococcales	0.80	0.83	-0.76	0.26	-0.06	-0.72
2-Week Time-Series	"*Ca.* Methanoperedens"	-0.88	-0.58	-0.47	-0.92	-0.68	0.73
	ANME-1	0.89	0.60	0.46	0.91	0.69	-0.75
	Methylococcales	n.a.	n.a.	n.a.	n.a.	n.a.	n.a.

Table 4: **Correlation (Pearson's r) between taxa RNA abundance (determined by PEG abundance) and geochemical parameters**. The R^2_{mcrA} values reported in the main text are the square of the values reported above. n.a. = not applicable; *Correlations of *Methylococcales* and geochemical parameters were not calculated as *Methylococcales*-related *mmo* were below detection during T_0 and T_1.

1, "Ca. Methanoperedens", and *Methylococcus* are best described as a SO_4^{2-}-dependent ANME[15], NO_3^--dependent ANME[20], and aerobic methanotrophs[21], respectively, we designed experiments to test whether or not each MO-lifestyle would respond to an increase in the aforementioned electron acceptor. The first experiment (Experiment 1) was a long-term experiment analyzed over 207[2] days and contained fracture fluid samples from 2012 and 2013 enriched with either ^{13}C-CH_4 (Control A), ^{13}C-CH_4+SO_4^{2-} (to stimulate ANME-1), or ^{13}C-CH_4+NO_3^- (to stimulate "Ca. Methanoperedens"). A second set of 2012 and 2013 fracture fluid enrichments (Experiment 2) were analyzed as a short-term experiment for 43 days. Experiment 2 contained ^{13}C-CH_4 treatments of ^{13}C-CH_4+paraformaldehyde (4%, v/v) (Control B), ^{13}C-CH_4+SO_4^{2-}, ^{13}C-CH_4+O_2, and ^{13}C-CH_4+NO_3^- as well as an electron acceptor- and donor- free control (Control C). Unlike the correlations observed

[2]The long term ^{13}C-CH_4+NO_3^- enrichments were run for 183 days.

between expression data and geochemical parameters, an increase in the proportion of ^{13}C-CO_2 relative to total CO_2 ($\%^{13}$C-CO_2) in the $^{13}CH_4$ enrichments over time is definitive evidence of $^{13}CH_4$ oxidation under different conditions.

In Experiment 1, the ^{13}C-CH_4+NO_3^- enrichments exhibited the greatest rate of $\%^{13}$C-CO_2 production and, in 2012, the rate of $\%^{13}$C-CO_2 production (0.017 ± 0.005 $\%^{13}$C-CO_2 day^{-1}) was found to be significantly greater (paired one-tailed Student t-test; $p = 0.02$) than Control A (0.004 ± 0.001 $\%^{13}$C-CO_2 day^{-1}) (Figure 3). No enrichments from Experiment 2 exhibited an increase in $\%^{13}$C-CO_2 production (Supplementary Data 5). Although ANME-1 was present in the metatranscriptomic and metaproteomic data during the 2012 and 2013 sampling points, there was not a significant difference in $\%^{13}$C-CO_2 production between Experiment 1's ^{13}C-CH_4+SO_4^{2-} enrichments and Control A (Figure 3). This similarity may be best explained by either SO_4^{2-} driven AOM in Control A or trace CH_4 oxidation during methanogenesis[22]. Notably, the concentrations of SO_4^{2-} in Controls A, B, and C ($[SO_4^{2-}{}_{2012}] = 623$ μM; $[SO_4^{2-}{}_{2013}] = 479$ μM) are well within the lower range of SO_4^{2-} concentrations (100-1200 μM) that have been reported for SO_4^{2-} coupled AOM[23]. Furthermore, the 2012 Control C samples (Experiment 2) exhibited net CH_4 oxidation ($\Delta[CH_4] = -0.14 \pm 0.08$ mM) suggestive of SO_4^{2-} coupled AOM. On the other hand, the 2013 Control C exhibited net CH_4 production ($\Delta[CH_4] = 0.11 \pm 0.01$ mM); however, the rate of observed methanogenesis is probably too low to be responsible for the elevated rates of $\%^{13}$C-CO_2 production that would occur as a result of trace methane oxidation. Therefore, the $\%^{13}$C-CO_2 production in the ^{13}C-CH_4+SO_4^{2-} enrichments of Experiment 1 are most likely explained by SO_4^{2-} coupled AOM.

The lack of observable changes in the MO community and activity in the 2-week time series and the short-term enrichment experiments (Experiment 2), respectively, suggest that the this subsurface system has a slower microbial response to environmental change than other systems[24, 25, 26]. This finding is consistent with the perception that subsurface organisms spend their lives "in the slow lane." However, the significant increase in the rate of $\%^{13}$C-CO_2 production throughout the long-term ^{13}C-CH_4+NO_3^- enrichment experiments and the succession of MO organisms in the Be326 time series in coordination with changes in geochemistry illustrate a more dynamic subsurface ecosystem than previously understood.

METHOD SUMMARY

The Be326 borehole is a 57-m, horizontally drilled borehole. Be326 was drilled in 2007 and is located at the 26 level of the Beatrix Gold Mine (28.232288 S, 26.794365 E; Welkom, South Africa). Samples for this study were collected during field trips in 2011, 2012, and 2013. All other methods are described in the Supplement. Metagenomic and metatranscriptomic data are available at NCBI BioProject PRJNA308990. 16S amplicon data are available under NCBI BioProject PRJNA263371.

Acknowledgements

We would like to thank Sibanye Gold Ltd. and the staff of Beatrix Au Mine (Welkom, South Africa) for access and support in collecting subsurface samples. We thank G. Fournier for providing insight and computational support for this project. Subsurface research was funded by the National Geographic Society (BSL), National Science Foundation (NSF) (BSL, TLK, TCO, CM), Center for Dark Energy Biosphere Investigations (CM), and the Natural Sciences and Engineering Research Council of Canada (NSERC) (BSL, GFS). Any opinion, findings, and conclusions or recommendations expressed in this material are those of the authors and do not necessarily reflect the views of the National Science Foundation. Metagenome sequencing was supported by NASA EPSCoR/New Mexico Space Grant Consortium funding to TLK.

Supplementary Material

Supplementary Methods and Discussion along with the listed Supplementary Data are available on the BioArxiv website.

- Supplementary Data 1: Datasets used for protein mapping
- Supplementary Data 2: Assembled *mcrA* and *mmo* PEGs
- Supplementary Data 3: Predicted proteins from assembled *mcrA* and *mmo* PEGs
- Supplementary Data 4: Protein mapping results
- Supplementary Data 5: Enrichment experiment results
- Supplementary Data 6: McrA protein library used to generate phylogenetic tree
- Supplementary Data 7: Results of taxonomic profiling (referred to in Supplementary Discussion)

Figures

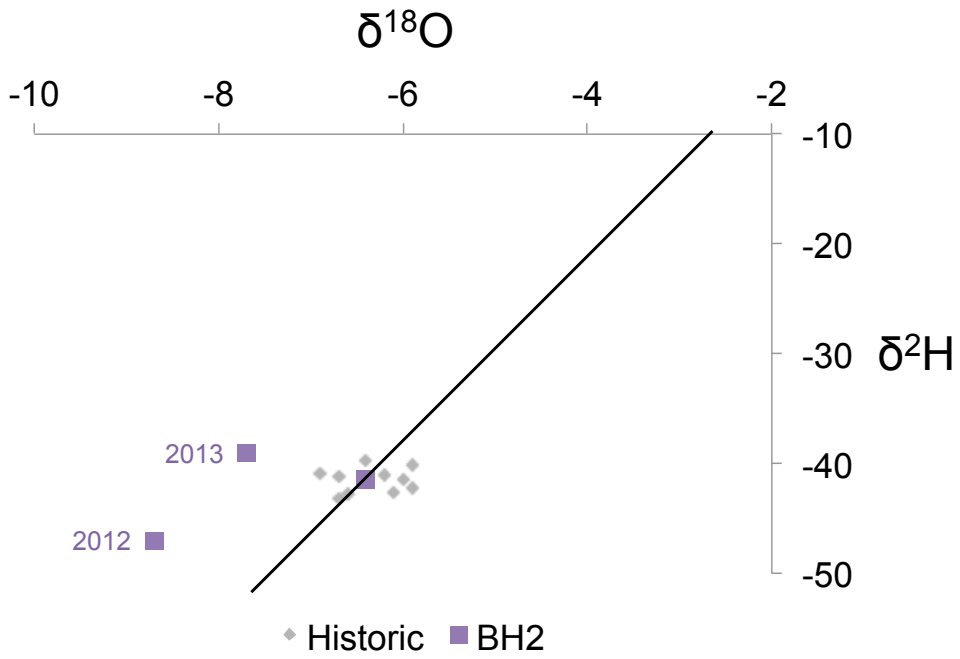

Figure 1: $\delta^2\mathbf{H}_{H2O}$ **and** $\delta^{18}\mathbf{O}_{H2O}$ **for Beatrix (Be) Gold Mine fracture fluids**. This figure plots the δ^{18}O (x-axis) against the δ^2H (y-axis) for each of the three time points (purple) in the long-term study of Be326 (2011, 2012, 2013). The diagonal black line represents the Global Meteoric Water Line[12] (GMWL). Gray diamonds represent historic data for Be adapted from Ward et al. (2004). The 2011 sample sits on the GMWL consistent with paleometeoric water[27, 28]. The 2012 and 2013 time points are displaced away from the GMWL along trends that have been observed to be consistent with mixing with older more saline fracture fluids[28, 1].

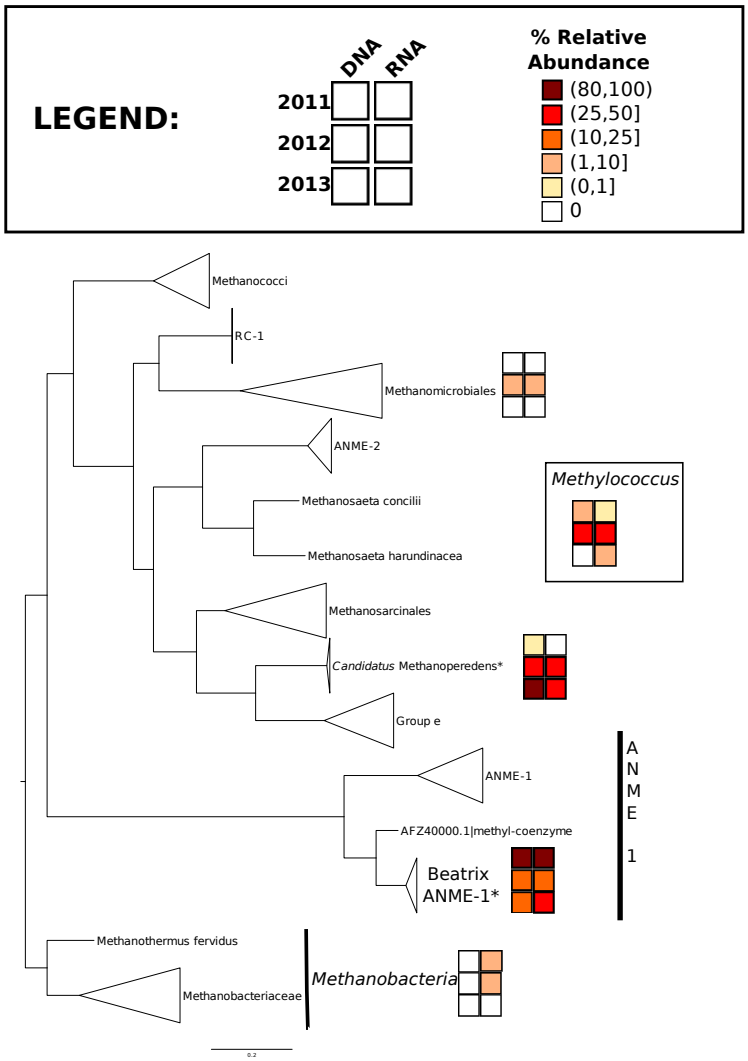

Figure 2: **Change in the CH_4 oxidizing community and activity over time**. A phylogenetic tree was constructed using PhyML[29] from a McrA peptide database (Supplementary Data 6) and the predicted proteins from the mcrA targeted assembly (designated by a $*$). The predicted MMO from the targeted assembly is also displayed. The 2×3 blocks represent the relative abundance of each taxa (DNA, left column; RNA, right column) with respect to their CH_4-related protein of interest (McrA or MMO) over time (row 1, 2011; row 2, 2012; row 3; 2013). Notably, Methanobacteria-related McrA PEGs were selected as the outgroup in this presentation of the McrA phylogenetic tree due to Methanobacteria's placement in species tree of Euryarchaeota.

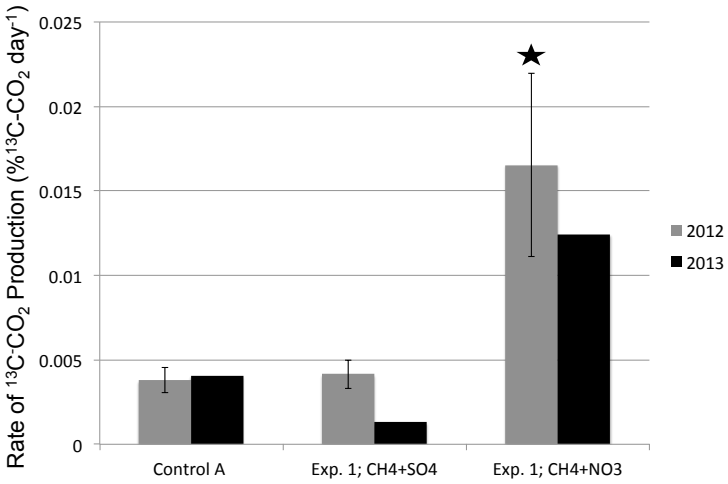

Figure 3: **^{13}C-CO$_2$ production after ^{13}C-CH$_4$ enrichment**.The rates of ^{13}C-CO$_2$ production (%^{13}C-CO$_2$ day^{-1}) from the 2012 (gray) and 2013 (black) fluids of Experiment 1 are displayed. The 2012 samples were run in triplicate and the standard deviations are shown. The star above the 2012 CH$_4$+NO3 bar indicates that the rate of ^{13}C-CO$_2$ production in the ^{13}C-CH$_4$+NO_3^- enrichment was significantly greater ($p = 0.02$) than the electron acceptor-free control (Control A).

References

[1] Sherwood Lollar, B. *et al.* Hydrogeologic controls on episodic H2 release from Precambrian fractured rocks-Energy for deep subsurface life on Earth and Mars. *Astrobiology* **7**, 971–986 (2007).

[2] Phelps, T. J., Murphy, E. M., Pfiffner, S. M. & White, D. C. Comparison between geochemical and biological estimates of subsurface microbial activities. *Microbial Ecology* **28**, 335–349 (1994).

[3] Whitman, W. B., Coleman, D. C. & Wiebe, W. J. Prokaryotes: the unseen majority. *Proceedings of the National Academy of Sciences of the United States of America* **95**, 6578–6583 (1998).

[4] D'Hondt, S., Rutherford, S. & Spivack, A. J. Metabolic activity of subsurface life in deep-sea sediments. *Science* **295**, 2067–2070 (2002).

[5] Lin, L.-H. *et al.* Radiolytic H2 in continental crust: nuclear power for deep subsurface microbial communities. *Geochemistry, Geophysics, Geosystems* **6** (2005).

[6] Schippers, A. *et al.* Prokaryotic cells of the deep sub-seafloor biosphere identified as living bacteria. *Nature* **433**, 861–864 (2005).

[7] Lomstein, B. A., Langerhuus, A. T., DHondt, S., Jørgensen, B. B. & Spivack, A. J. Endospore abundance, microbial growth and necromass turnover in deep sub-seafloor sediment. *Nature* **484**, 101–104 (2012).

[8] Onstott, T. C. *et al.* Does aspartic acid racemization constrain the depth limit of the subsurface biosphere? *Geobiology* **12**, 1–19 (2014).

[9] Magnabosco, C. *et al.* Comparisons of the composition and biogeographic distribution of the bacterial communities occupying South African thermal springs with those inhabiting deep subsurface fracture water. *Frontiers in microbiology* 679.

[10] Simkus, D. N. *et al.* Variations in microbial carbon sources and cycling in the deep continental subsurface. *Geochimica et Cosmochimica Acta* (2015).

[11] Onstott, T. C. *et al.* The origin and age of biogeochemical trends in deep fracture water of the Witwatersrand Basin, South Africa. *Geomicrobiology Journal* **23**, 369–414 (2006).

[12] Craig, H. Isotopic variations in meteoric waters. *Science* 1702–1703 (1961).

[13] Frape, S. K., Fritz, P. & McNutt, R. H. t. Water-rock interaction and chemistry of groundwaters from the Canadian Shield. *Geochimica et Cosmochimica Acta* **48**, 1617–1627 (1984).

[14] Ruby, J. G., Bellare, P. & DeRisi, J. L. PRICE: software for the targeted assembly of components of (meta) genomic sequence data. *G3: Genes— Genomes— Genetics* **3**, 865–880 (2013).

[15] Knittel, K. & Boetius, A. Anaerobic oxidation of methane: progress with an unknown process. *Annual review of microbiology* **63**, 311–334 (2009).

[16] McDonald, I. R., Bodrossy, L., Chen, Y. & Murrell, J. C. Molecular ecology techniques for the study of aerobic methanotrophs. *Applied and Environmental Microbiology* **74**, 1305–1315 (2008).

[17] Luton, P. E., Wayne, J. M., Sharp, R. J. & Riley, P. W. The mcrA gene as an alternative to 16S rRNA in the phylogenetic analysis of methanogen populations in landfill. *Microbiology* **148**, 3521–3530 (2002).

[18] Holmes, A. J., Costello, A., Lidstrom, M. E. & Murrell, J. C. Evidence that participate methane monooxygenase and ammonia monooxygenase may be evolutionarily related. *FEMS microbiology letters* **132**, 203–208 (1995).

[19] Langmead, B. & Salzberg, S. L. Fast gapped-read alignment with Bowtie 2. *Nature methods* **9**, 357–359 (2012).

[20] Haroon, M. F. *et al.* Anaerobic oxidation of methane coupled to nitrate reduction in a novel archaeal lineage. *Nature* **500**, 567–570 (2013).

[21] Kleiveland, C. R. *et al.* Draft genome sequence of the methane-oxidizing bacterium Methylococcus capsulatus (Texas). *Journal of bacteriology* **194**, 6626 (2012).

[22] Zehnder, A. J. & Brock, T. D. Methane formation and methane oxidation by methanogenic bacteria. *Journal of Bacteriology* **137**, 420–432 (1979).

[23] Segarra, K. E. A. *et al.* High rates of anaerobic methane oxidation in freshwater wetlands reduce potential atmospheric methane emissions. *Nature Communications* **6** (2015).

[24] Halet, D., Boon, N. & Verstraete, W. Community dynamics of methanotrophic bacteria during composting of organic matter. *Journal of bioscience and bioengineering* **101**, 297–302 (2006).

[25] Ho, A., Lüke, C. & Frenzel, P. Recovery of methanotrophs from disturbance: population dynamics, evenness and functioning. *The ISME journal* **5**, 750–758 (2011).

[26] Timmers, P. H. *et al.* Anaerobic oxidation of methane associated with sulfate reduction in a natural freshwater gas source. *The ISME journal* (2015).

[27] Lippmann, J. *et al.* Dating ultra-deep mine waters with noble gases and 36 Cl, Witwatersrand Basin, South Africa. *Geochimica et Cosmochimica Acta* **67**, 4597–4619 (2003).

[28] Ward, J. *et al.* Microbial hydrocarbon gases in the witwatersrand basin, south africa: implications for the deep biosphere. *Geochimica et Cosmochimica Acta* **68**, 3239–3250 (2004).

[29] Guindon, S. *et al.* New algorithms and methods to estimate maximum-likelihood phylogenies: assessing the performance of PhyML 3.0. *Systematic biology* **59**, 307–321 (2010).